Journal of Applied Mechanics and Technical Physics, Vol. 45, No. 4, pp. 510–516, 2004

EFFECT OF FREE-STREAM TURBULENCE ON THE FLOW STRUCTURE NEAR A WEDGE AND THE WINDWARD SIDE OF AN AIRFOIL

A. P. Brylyakov, G. M. Zharkova, B. Yu. Zanin, V. N. Kovrizhina, and D. S. Sboev

UDC 536.244

The flow structure behind wire grids is studied for flows with a low subsonic velocity, and the effect of grids on the boundary-layer flow structure is considered. It is shown that the mean-velocity inhomogeneity induced by the grid does not disappear until a distance of 925 calibers downstream of the grid is reached. Liquid-crystal thermography combined with hot-wire measurements made it possible to find the source of steady large-scale streamwise vortex structures in the boundary layer on a wedge and on an airfoil and to determine the parameters of these structures.

Key words: *grids, airfoil, wedge, boundary layer, hot-wire anemometry, liquid-crystal thermography.*

Introduction. To describe free-stream perturbations caused by turbulence, the energy, spectral, and scale characteristics of the latter are used [1, 2]. In most papers, the effect of the turbulence level on the flow structure is considered, whereas the role of, e.g., free-stream velocity inhomogeneities or macroscale of turbulence has not been adequately studied [2–9]. In practice, the isolated influence of the elevated level of turbulence is rarely observed; therefore, combined effects are often studied. Thus, for a given level of turbulence, it is possible to achieve superposition of a well-controlled distribution of mean velocity by means of turbulence generators. The controlled mean free-stream velocity distribution or streamwise vorticity is generated by grids, perforated screens, winglets, etc.

The present work continues the study of the influence of disturbances generated by wire grids on the flow structure in the boundary layer on an airfoil and in a constricted channel [10]. Though grids are used in tranquilization chambers of wind tunnels to reduce flow inhomogeneities and damp the "incoming" turbulence, they can introduce their own inhomogeneities into the flow. Obtaining reliable information on parameters of the internal structure of free-stream turbulence can refine the notions on dominating mechanisms in various flows. The effects of moderately elevated turbulence (Tu $\approx 1\%$) typical, in particular, of flows behind grids are considered in the present paper. The interest in this problem is caused by the development of methods for controlling subsonic flows, solving problems of the transport theory in turbulized flows, monitoring and improvement of flow quality in wind tunnels, etc.

The effects of an inhomogeneous distribution of free-stream velocity have been most adequately studied for a flow past a flat plate, where these effects are manifested as a streaky structure similar to that observed in the case of elevated free-stream turbulence [8]. In contrast to the flow past a flat plate, where the streaky structures are commensurable with the boundary-layer thickness and are unsteady, the influence of an inhomogeneous distribution of free-stream velocity in the Hiemenz flow, near the stagnation point on a circular cylinder, is manifested in the form of steady large-scale streamwise structures with a relative wavelength $\lambda/\delta \gg 1$. To explain the origination of these

Institute of Theoretical and Applied Mechanics, Siberian Division, Russian Academy of Sciences, Novosibirsk 630090. Translated from Prikladnaya Mekhanika i Tekhnicheskaya Fizika, Vol. 45, No. 4, pp. 64–71, July–August, 2004. Original article submitted June 24, 2003; revision submitted September 23, 2003.

TABLE 1

Parameters of Grids and Flow Regimes

Grid number	M, mm	d, mm	Tu, % ($x = 350$ mm)	Re_d ($U = 6$ m/sec)
1	1	0.25	0.7	224
2	2	0.4	1	320
3	5.5	1.2	1.8	576

Note. M is the cell size and d is the wire diameter.

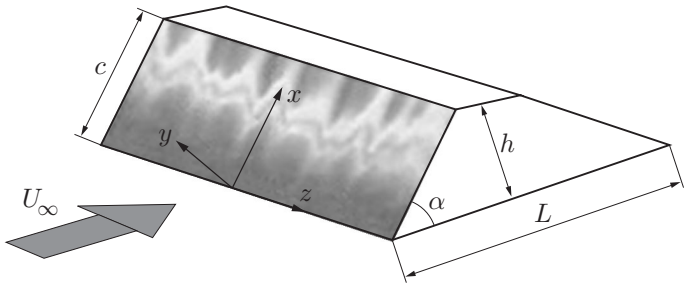

Fig. 1. Wedge configuration and fragment of LC visualization of the temperature field (the transverse size of the visualization pattern was 120 mm; grid No. 2, $U_\infty = 6$ m/sec; $\alpha = 45°$; the distance from the grid was $x_1/M = 175$).

structures, Sutera et al. [9] proposed a mathematical model for studying the mechanism of vorticity amplification, caused by extension of streamwise vortices in the divergent flow in the stagnation region. It was shown [9] that the flow pattern observed on a circular cylinder is directly related to free-stream inhomogeneity and does not result from boundary-layer instability at the stagnation point of the flow.

The objective of the present work is to experimentally study the generic features of the flow around a wedge and a curved airfoil (noncircular cylinder) under a combined action of elevated turbulence and low inhomogeneity of the free-stream flow, and also to refine the mechanisms of influence of these factors. To confine the consideration to an attached flow, we consider the flow only on the windward side of the airfoil at angles of attack $\alpha = 0$–$27°$.

1. Test Conditions and Methods of Research. 1.1. *Experimental Facilities and Models.* The first set of experiments was performed in an MT-324 subsonic wind tunnel of the Institute of Theoretical and Applied Mechanics (ITAM) of the Siberian Division of the Russian Academy of Sciences . The test section of the wind tunnel was $200 \times 200 \times 700$ mm. The level of free-stream turbulence in the closed test section of the wind tunnel was $\mathrm{Tu} = u'/U_\infty = 0.1\%$. Wire grids were used to increase the turbulence level. The parameters of the grids used are listed in Table 1. A widely used configuration modeling a confuser was used, namely, a wedge-shaped step with a sharp leading edge, which was made of wood and whose width was equal to the width of the test section (Fig. 1). In the streamwise section, the step had a form of a trapezium with a base length $L = 168$ mm, height $h = 50$ mm, and angles of inclination of the side faces of 30 and 45° (leading and trailing edges). The experiments were performed for Reynolds numbers $\mathrm{Re}_h = 1.3 \cdot 10^4$ and $2 \cdot 10^4$ based on the step height and $\mathrm{Re}_L = 4.48 \cdot 10^4$ and $6.72 \cdot 10^4$ based on the base length.

The second set of experiments was performed in a T-324 subsonic wind tunnel (ITAM), which is characterized by a better quality of the flow, in particular, better stability of the mean free-stream velocity in time and initial level of turbulence $\mathrm{Tu} = 0.04\%$. The test-section size is $1000 \times 1000 \times 4000$ mm. To increase the level of turbulence, we used a grid with a mesh size of 2×2 mm, which was identical to grid No. 2 (see Table 1). The flow on the windward side of a low-aspect-ratio straight wing was considered. The model of a symmetric airfoil with a wing chord $c = 228$ mm, span of 311 mm, and relative thickness of 15% was made of wood. To prevent lateral spillage, tip washers were used. The experiments were performed for a Reynolds number based on the wing chord $\mathrm{Re}_c = 1.76 \cdot 10^5$.

1.2. *Method of Liquid-Crystal Thermography* (LCT). Liquid-crystal (LC) indicator films were used for panoramic visualization and temperature-field measurement [11]. Owing to the small thickness of the films (about 25 μm), the presence of the temperature-sensitive film does not disturb the temperature field considered. The temperature-measurement procedure consisted in determining the color coordinates in the HSI space for each point of the wing surface and subsequent digitizing of results with the use of the calibration dependence of temperature on the hue. A detailed description of the method can be found in [12].

In the experiments, we used LC coatings with a 3°C width of the selective reflection band and boundary conditions of the second kind (constant heat-flux density on the model surface). The heat-flux inhomogeneity was monitored by the color of the LC coating in experiments without the flow and did not exceed 10% along the model edges.

1.3. *Hot-Wire Anemometry.* In the course of the experiment, the mean (U) and fluctuating (u') components of streamwise velocity were measured by a constant-temperature anemometer with a single-wire probe. The electric signals were measured by a bridge of a 55M01 DISA hot-wire anemometer. Through a substractor (unit of d.c. voltage shifting for expanding the dynamic range) and a MacADIOS-Adio analog-to-digital converter produced by GW Instruments, the digitized signals were fed to a Macintosh Classic II personal computer produced by Apple Computers for subsequent processing. The length and diameter of the tungsten wire in the hot-wire probe were 1 mm and 6 μm, respectively. The calibration was performed in the free stream near a Pitot–Prandtl tube with flow velocities of 2–12 m/sec for MT-324 and 2–20 m/sec for T-324. The error in determining the mean velocity was less than 3% for measurements in the boundary layer on the wedge (U = 2–3 m/sec) and 1% for measurements in the free stream in the T-324 wind tunnel for $U \approx 12$ m/sec.

2. Test Results. 2.1. *Structure of the Near-Wall Flow on a Wedge.* In the first set of experiments, we considered the boundary-layer structure on a wedge. Smoke visualization showed that a flow with a divergence line is formed on the wedge. It follows from the results of LC visualization of the temperature field that steady streamwise structures are formed in the boundary layer on the wedge if a grid is mounted at the nozzle exit; these structures are manifested as alternating bands of elevated and reduced surface temperature with a certain characteristic transverse scale (see Fig. 1). The location and size of these structures are independent of the test duration and are reproduced in repeated experiments.

To clarify the degree of correspondence between LC visualization and the real structure of the boundary layer, we performed hot-wire measurements with grid No. 2 (U_∞ = 6 m/sec, $\alpha = 45°$, and $x_l/M = 175$). The measurements in the boundary layer on the wedge showed that the mean streamwise velocity in the spanwise direction is modulated with an amplitude reaching 20% of local velocity. A similar modulation is observed for root-mean-square fluctuations of the streamwise component of velocity in the boundary layer; the temperature maximums and minimums correspond to the regions of low and high fluctuations of velocity, respectively. The displacement thickness also depends on the transverse coordinate and is greater in the valley. Figures 2 and 3 show the isolines of the mean velocity and velocity fluctuations in the plane yz in the cross section $x/c = 0.42$ (c is the length of the lateral face of the wedge), which reveal the presence of four peaks and valleys in the measurement region. The measurement data allow us to assume that the boundary-layer structure is a system of counterrotating vortices with the transverse size several times greater than the boundary-layer thickness. The process of formation of such vortices near the stagnation line, which are outside the laminar boundary layer, was considered, e.g., in [13].

2.2. *Effect of Test Geometry and Free-Stream Velocity on the Structure of the Near-Wall Flow Around a Wedge.* To find the regular features determining the transverse scale of streamwise structures, LC thermography was performed for two wedge angles $\alpha = 30°$ and $\alpha = 45°$ and velocities U_∞ = 4 and 6 m/sec with an unchanged location of grid No. 2. It was found that the number of bands on visualization patterns and the coordinates of peaks and valleys on temperature curves coincide for all parameters considered. The same result is obtained if the distance between the grid and the leading edge of the model is increased from $x_l/M = 175$ to 213. The discrete Fourier transform (DFT) of the transverse distribution of temperature shows that, with accuracy to the minimum frequency resolution of DFT, the maximums for all examined values of the wedge angle, free-stream velocity, and distance between the grid and the leading edge correspond to the wavelength $\lambda = (17 \pm 2.4)$ mm.

LC visualization and plots of DFT of temperature curves obtained with the use of three different grids showed that the transverse wavelength of the streamwise structures with accuracy to the minimum resolution is (17 ± 2) mm for grid Nos. 1 and 2; this value is much higher for grid No. 3 and reaches (37 ± 12) mm.

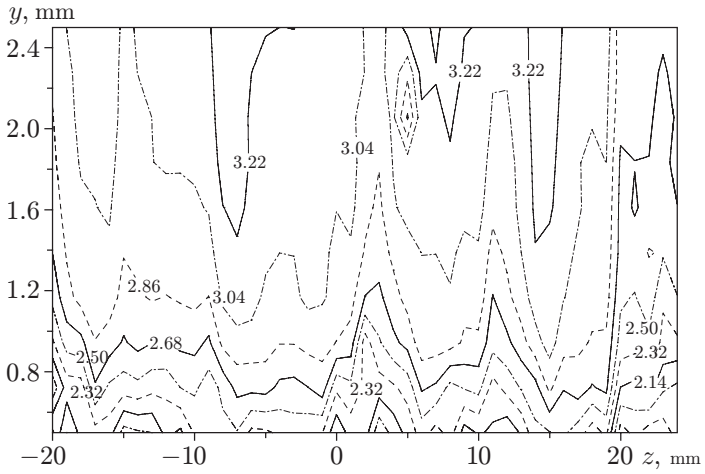

Fig. 2. Isolines of mean velocity (m/sec) in the plane (yz) in the cross section $x/c = 0.42$ for $x_1/M = 175$.

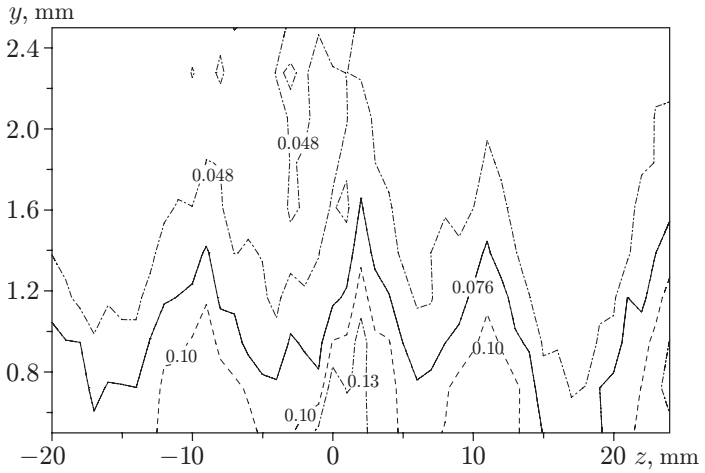

Fig. 3. Isolines of fluctuations of the streamwise component of velocity u' in the plane (yz) in the cross section $x/c = 0.42$ for $x_1/M = 175$.

A comparison revealed good agreement between LCT and hot-wire results: the scales of the structures coincide; regions with a high mean velocity correspond to regions with low temperature, and vice versa. In addition, it was found that methodical overheating of the surface by 10–15°C does not affect the transverse scale of the structures.

Based on the test results, we can assume that the leading role in formation of spatial structures in this flow belongs to the structure of free-stream disturbances generated by the grid.

3. Flow Structure behind the Turbulizing Grid in the Absence of the Model. To clarify the physical mechanism responsible for origination of streamwise structures, the parameters of the flow behind a turbulizing grid were studied in the T-324 wind tunnel; the mesh size and wire diameter in this grid corresponded to those of grid No. 2 used previously. The mean velocity was measured without the model; the probe was moved in space along the line corresponding to the position of the leading edge of the model. It turned out that the mean velocity and root-mean-square fluctuations are not constant along the z coordinate. Alternation of regions with elevated and reduced mean velocity of the flow is observed. The maximum scatter of the mean velocity ($\Delta U_{\max}$) and the level of velocity fluctuations averaged over the cross section ($\bar{u}'$) are listed in Table 2. It is seen from Table 2 that the flow is not homogeneous even at a distance $x_l/M = 925$ behind the grid.

TABLE 2

Parameters of the Flow behind Grid No. 2 ($U = 12$ m/sec)

x, mm	x/M	$\Delta U_{\max}/U$, %	$\bar{u}'$, %
350	175	8	0.89
850	425	7.1	0.60
1850	925	5.7	0.53

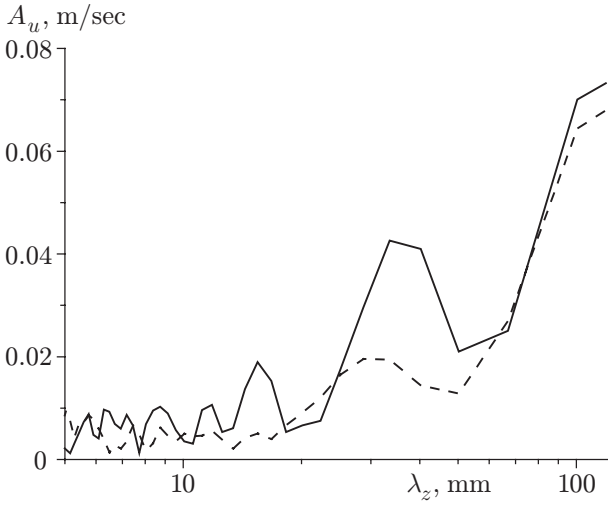

Fig. 4

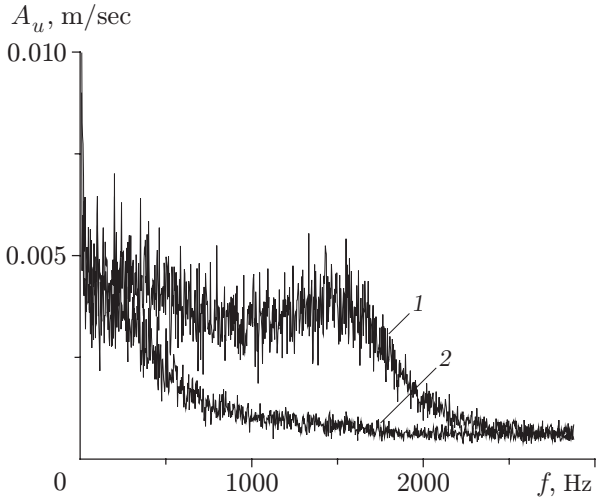

Fig. 5

Fig. 4. Discrete Fourier transform of the mean streamwise velocity in the free stream behind the grid: the dashed and solid curves refer to $x_1/M = 175$ and 925, respectively.

Fig. 5. Spectra of fluctuations of the streamwise component of velocity in the free stream behind the grid: $x_1/M = 175$ (1) and 925 (2).

The evolution of the transverse scale of streamwise structures in the free stream with increasing distance between the grid and the probe can be easily seen from the plots of the spatial Fourier transform of the mean velocity for $x_l/M = 175$ and 925 (Fig. 4). It is seen that the amplitudes of the second harmonic of disturbances (velocity A_u and temperature A_T) strongly decrease with increasing distance. The character of the spectrum of fluctuations of the streamwise velocity also changes (Fig. 5) toward decreasing amplitude of high-frequency components.

4. Flow Structure on the Windward Side of an Airfoil. LC visualization showed that the streamwise structures are not observed in the boundary layer on the airfoil without the grid, as in the case with the wedge. When the grid was mounted, the structures appeared at a distance of 175–925 calibers from the leading edge of the model. The characteristic transverse size of the structures in this case is about 18 mm, which is in good agreement with the scale of the structures on the wedge (17 mm), for grid No. 2.

4.1. *Effect of the Distance Between the Grid and the Leading Edge of the Model* ($\alpha = 27°$). A comparison of results of DFT of the transverse distributions of velocity and temperature on the model surface with an identical distance between the grid and the probe and between the grid and the leading edge showed (Fig. 6) that there are two spatial scales corresponding to two highest peaks of spectral power density both in the flow and on the model at a distance of 175 calibers from the grid. The first peak [$\lambda_z = (44 \pm 14)$ mm] corresponds to the period of the observed modulation of the mean velocity; the second peak [$\lambda_z = (17 \pm 2.4)$ mm] refers to the streamwise structures registered by LC visualization. The high value of amplitude for frequencies close to zero is, apparently, caused by the fact that the mean velocity profile has a certain slope, which leads to appearance of low-frequency components in DFT. As the distance from the grid to the leading edge increases to $x_l/M = 925$, the small-scale structures ($\lambda_z = 17$ mm) disappear, and the large-scale structures ($\lambda_z = 44$ mm) remain.

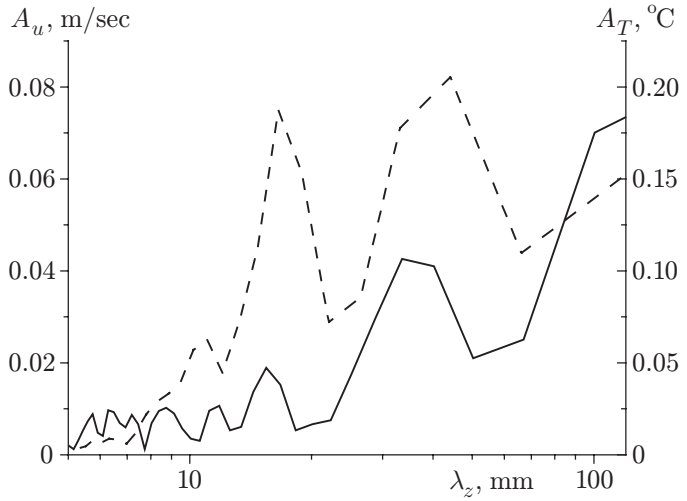

Fig. 6. Discrete Fourier transform of the transverse distribution of velocity (solid curve) and temperature (dashed curve) on the model surface ($x_1/M = 175$).

The agreement between the spatial structure of the boundary layer and the spatial structure of disturbances generated by the grid, apparently, testifies that the mechanism of vorticity extension is responsible for origination of streamwise structures. A similar phenomenon is also observed for an angle of attack of the airfoil $\alpha = 0$. Among the entire set of experiments performed, this case is most close to the flow around a cylinder considered in [14], where the formation of streamwise vortices near the leading edge of a blunted body by means of extension of vorticity of steady inhomogeneities in the free stream was studied.

A change in the angle of attack does not involve any significant changes in the transverse wavelength, though a shift of the peak corresponding to the wavelength of streamwise structures by the value of the minimum frequency resolution of DFT is observed in the plots of DFT of temperature corresponding to different angles of attack.

Thus, the bodies considered in the present paper, apparently, do not generate instabilities near the divergence lines but only display the spatial structure of disturbances incoming from the ambient flow.

Conclusions. The results on the structure of near-wall flows arising on the windward side of an airfoil and a wedge under a combined action of elevated turbulence and transverse gradient of free-stream velocity induced by wire grids are described in the paper.

It is found that the influence of free-stream disturbances in the boundary layer on the wedge in the MT-324 wind tunnel is manifested as a system of steady streamwise structures with a characteristic transverse size λ, which is several times greater than the boundary-layer thickness δ. The location of these structures and the value of λ are determined by the grid. Changes in the wedge angle ($\alpha = 30$ and $45°$), distance from the grid (175–213 calibers), and free-stream velocity ($U_\infty = 4$ and 6 m/sec) do not affect the flow structure. At the same time, small modulations of the mean free-stream velocity with an amplitude of 1–2% have a significant effect on the boundary-layer structure: the velocity defect in the boundary layer on the wedge due to the streamwise structures reaches 20%.

The structure of the free stream behind a turbulizing grid and in the boundary layer on an airfoil with a chord-based Reynolds number of $1.76 \cdot 10^5$ was studied in the T-324 wind tunnel. The transverse distribution of mean free-stream velocity and root-mean-square fluctuations behind the grid was found to be inhomogeneous. Their characteristics as functions of the distance from the grid were determined. Good agreement between the transverse scales of the structures in the boundary layer on the airfoil and the transverse scales of grid-induced disturbances of the mean free-stream velocity is demonstrated by methods of LCT and Fourier analysis. Good agreement between the data of LC thermography and hot-wire anemometry demonstrates the effectiveness of using liquid-crystal visualization in studying near-wall flows.

This work was supported by the Russian Foundation for Basic Research (Grant Nos. 01-01-00828 and 04-01-00154) and by the Integration Project No. 25 of the Siberian Division of the Russian Academy of Sciences.

REFERENCES

1. P. Bradshaw, *An Introduction to Turbulence and its Measurement*, Pergamon Press, Oxford (1971).
2. E. P. Dyban and É. Ya. Épik, *Heat and Mass Transfer and Hydrodynamics of Turbulized Flows* [in Russian], Naukova Dumka, Kiev (1985).
3. J. Böttcher and E. Wedemeyer, "The flow downstream of screens and its influence on the flow in the stagnation region of cylindrical bodies," *J. Fluid Mech.*, **204**, 501–522 (1989).
4. W. S. Saric, E. B. White, and H. L. Reed, "Boundary-layer receptivity to free-stream disturbances and its role in transition," AIAA Paper No. 99-3788 (1999).
5. K. J. A. Westin, A. V. Boiko, B. G. V. Klingman, et al., "Experiments in a boundary layer subject to free-stream turbulence. Part 1: Boundary layer structure and receptivity," *J. Fluid Mech.*, **281**, 193–218 (1994).
6. D. L. Rigby and G. J. Van Fossen, "Increased heat transfer to a cylindrical leading edge due to spanwise variation in the free-stream velocity," AIAA Paper No. 91-1739 (1991).
7. G. J. Van Fossen and Y. Ching Chang, "Measurements of the influence of integral length scale on stagnation region heat transfer," NASA TM-106503 (1994).
8. M. V. Ustinov, "Receptivity of the boundary layer on a flat plate with a blunted leading edge to steady nonuniformity of the free stream," *J. Appl. Mech. Tech. Phys.*, **41**, No. 4, 658–665 (2000).
9. S. P. Sutera, P. F. Maeder, and J. Kestin, "On the sensitivity of heat transfer to free stream vorticity," *J. Fluid Mech.*, **16**, 497–520 (1963).
10. G. M. Zharkova, B. Yu. Zanin, V. N. Kovrizhina, and A. P. Brylyakov, "Free stream turbulence effect on the flow structure over the finite span straight wing," *J. of Visual. Jpn.*, **2**, No. 5, 169–176 (2002).
11. G. M. Zharkova and A. S. Sonin, *Liquid-Crystal Composites* [in Russian], Nauka, Novosibirsk (1994).
12. G. M. Zharkova, V. N. Kovrizhina, and V. M. Khachaturyan, "Experimental study of subsonic flows by liquid-crystal thermography," *J. Appl. Mech. Tech. Phys.*, **43**, No. 2, 274–279 (2002).
13. S. D. R. Wilson and J. Gladwell, "The stability of two-dimensional stagnation flow to three-dimensional disturbances," *J. Fluid Mech.*, **84**, Part 3, 517–527 (1978).
14. W. Z. Sadeh, S. P. Sutera, and P. F. Maeder, "Analysis of vorticity amplification in the flow approaching a two-dimensional stagnation point," *Z. Angew. Math. Phys.*, **21**, 669–716 (1970).